Available online at www.sciencedirect.com

SciVerse ScienceDirect

Ceramics International 39 (2013) 4723–4727

CERAMICS INTERNATIONAL

www.elsevier.com/locate/ceramint

Short communication

Fabrication and properties of 3-D C_f/ZrC–SiC composites by the vapor silicon infiltration process

Qinggang Li[a,*], Shaoming Dong[b], Zhi Wang[a], Guopu Shi[a]

[a]*School of Material Science and Engineering, University of Jinan, Jinan 250022, China*

[b]*Structural Ceramics and Composites Engineering Research Center, Shanghai Institute of Ceramics, Chinese Academy of Sciences, Shanghai 200050, China*

Received 5 September 2012; received in revised form 8 November 2012; accepted 9 November 2012
Available online 16 November 2012

Abstract

Three-dimensional needled C_f/ZrC–SiC composites were successfully fabricated by the vapor silicon infiltration process. The bulk density, open porosity, and flexural strength of the composite with PyC/SiC interphases were 2.25 g/cm^3, 6%, and 301 MPa, respectively. All composites exhibited a non-brittle failure behavior due to propagation and deflection of cracks, as well as fracture and pullout of fibers. The mass loss and linear recession rate of the three-dimensional needled C_f/ZrC–SiC composite exposed to oxyacetylene torch were 0.013 g/s and 0.004 mm/s, respectively. The formation of $ZrSiO_4$ melt on the surface of the composite contributed mainly to the excellent high-temperature property of the composite.

Keywords: Vapor silicon infiltration; C_f/ZrC–SiC composites; High-temperature property

1. Introduction

With the demand for application of thermal protection systems, such as rocket nozzles, nosetip, aeronautic jet engines, and leading edges [1,2], carbon fiber-reinforced ultra-high temperature ceramic matrix (C_f/UHTC) composites have received considerable attention because of their unique physicochemical and mechanical properties. They have been widely used in high-temperature structural elements for aerospace equipments, and can withstand ablation environment with high heat flux and high pressure gas flows because of their high melting points, good thermal-shock resistance and superior ablation/oxidation resistance [3,4].

Continuous fiber-reinforced ceramic matrix composites were fabricated via chemical vapor infiltration (CVI), polymer impregnation and pyrolysis (PIP), reaction sintering (RS), hot pressing, and so on. Compared with CVI and PIP, RS is a more cost effective method for the fabrication of ceramic matrix composites (CMCs). However, RS involves reactive melt infiltration or liquid silicon infiltration (LSI) [5,6]. LSI has been mostly limited to the fabrication of biomorphic SiC ceramics [7]. Molten silicon infiltration has two drawbacks: reaction choking and flaw generation [8]. However, silicon vapor infiltration has the advantage of infiltrating smaller pores compared with molten silicon infiltration. Furthermore, it can be controlled to avoid reaction choking because of the slow reaction between silicon vapor and carbon [9]. Zhou et al. [9] fabricated carbon fiber-reinforced silicon carbide (C/SiC) composites using the vapor silicon infiltration (VSI) process and obtained dense C/SiC composites.

At present, zirconium carbide (ZrC) is widely used for the fabrication of C_f/UHTC composites. Our previous study focused on the fabrication of C_f/ZrC–SiC composites using ZrC precursor and polycarbosilane [10]. Other techniques for the fabrication of C_f/ZrC–SiC composites have been summarized in our work [11]. Thus far, studies on C_f/ZrC–SiC composites manufactured through VSI are lacking.

Based on our previous experience, the present work aims to develop a new technique for the fabrication of three-dimensional (3-D) C_f/ZrC–SiC composites. In this communication, we report our initial studies on the preparation of

*Corresponding author.
E-mail address: liqinggang66@gmail.com (Q. Li).

0272-8842/$ - see front matter
http://dx.doi.org/10.1016/j.ceramint.2012.11.024

3-D C_f/ZrC–SiC composites using vapor silicon infiltration. The mechanical and high-temperature properties of the 3-D C_f/ZrC–SiC composites obtained were studied.

2. Experimental procedure

Carbon fibers (T300SC, Toray, Tokyo, Japan) with an average diameter of 6 μm were used. The three-dimensional (3D) fabrics were fabricated by the Nanjing Fiberglass Research and Design Institute (Nanjing, China). The architecture had a fiber distribution of 8:2:1 in the *x*:*y*:*z* directions, respectively, and an ~40% fiber volume fraction. According to our previous study [9], a carbon layer (PyC: ~150 nm) was firstly deposited on the surface of the carbon fibers to serve as an interfacial layer. The layer was deposited by chemical vapor deposition (CVD) using methane as a precursor. Then, a 250 nm SiC layer was deposited by CVD, using MTS/H_2 precursor, to protect the fibers from reacting with the silicon vapors. Commercially available ZrC particles (Kaier Nanometer Technology Development Co. Ltd., Hefei, China) were balled with a phenolic resin (Shanghai Qinan Adhesive Material Factory, Shanghai, China) at a certain ratio, using ethyl alcohol as solvent to form homogenously dispersed slurry. Then the fabrics were impregnated by the aforementioned slurry, followed by pyrolysis at 900 °C to form a porous body (C_f/ZrC–C composites). The slurry infiltration process was performed in a vacuum, and then a pressure of 2 MPa was applied by nitrogen gas to facilitate the infiltration process. The pyrolyzed body contained a carbon matrix, ZrC, and a distribution of microspores. Such composites contained large number of pores and cracks. In order to fabricate C_f/ZrC–SiC composites by the VSI process, a silicon powder (purity: 99.9%, grain size: 75 μm, Sinopharm Chemical Reagent Co. Ltd., Shanghai, China) was put inside a graphite crucible, then the C_f/ZrC–C composites. Finally, the graphite crucible with silicon powder and C_f/ZrC–C composite were sealed and heated up to 1700 °C for 1.5 h in vacuum (residual pressure ~1 Pa). The gaseous Si penetrated into the porous channel and concurrently facilitated the reaction to form SiC. As a result, the 3-D C_f/ZrC–SiC composite was fabricated.

The densities of the samples were measured using Archimedes' method in water after evacuating the air from porosity. The samples were cut into 4 mm × 5 mm × 60 mm specimens and polished for three-point bending test. The flexural strength was measured by the three-point bending test in an Instron-5566 (Instron Corp., Canton, MA) universal testing machine, with a crosshead speed of 0.5 mm/min and a span of 48 mm. Young's modulus was calculated from the date recorded during three-point bending testing [12].

The phase compositions of the composites were characterized by X-ray diffraction (XRD, Mode: RAX-10, Rigaku, Japan) with Cu K_a radiation. The microstructures of the composites were studied by Electron Probe Micro-analyzer (EPMA, JXA-800, Jeol, Tokyo, Japan).

The oxidation resistance of the composites was evaluated by static oxidation at 1700 °C for 15 min in a muffle furnace. The anti-ablation property test was conducted in a flowing oxyacetylene torch environment. During the test, a specimen with a size of 80 mm × 80 mm × 10 mm was vertically exposed to the flame for 600 s when the surface temperature of the composite reached 1800 °C. The distance between the nozzle tip and the surface of the specimen was 10 mm and the inner diameter of the nozzle tip was 2.0 mm.

3. Results and discussions

The density and open porosity of the 3-D C_f/ZrC–SiC composite with PyC/SiC interphase before and after VSI are shown in Table 1. It can be seen that there are obvious differences observed among the composites before and after VSI. After VSI the bulk density of the composite increased from 1.77 g/cm^3 to 2.25 g/cm^3, whereas its open porosity decreased from 24% to 6%. By comparison, it is concluded that open porosities provide channels for the VSI process. Due to the VSI process, the density increased and open porosity decreased. During the VSI process, silicon vapor entered into the channels and the reaction generated SiC filled open porosities. On the whole, VSI can be considered as a suitable method for fabrication of dense composites, which is the same as our previous work [13]. In order to guarantee the VSI process smoothly and the amount of SiC matrix formed by the reaction between

Table 1
Density and open porosity of 3-D C_f/ZrC–SiC composite with PyC/SiC interphase before and after VSI.

Sample	Density (g cm^{-3})	Open porosity (%)
C_f/ZrC–C	1.77	24
C_f/ZrC–SiC	2.25	6

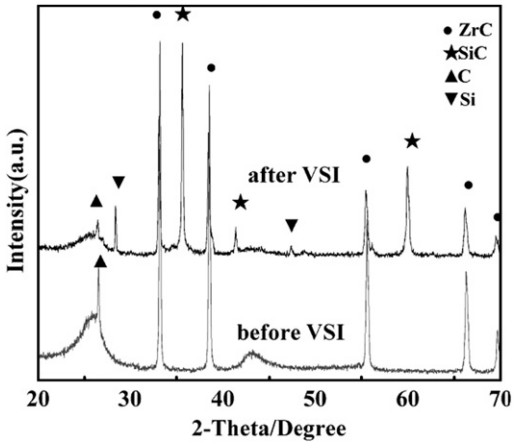

Fig. 1. XRD patterns of 3-D C_f/ZrC–SiC composites with PyC/SiC interphase before and after VSI.

silicon and carbon, the open porosity before VSI is controlled about 20%.

The XRD patterns of the 3-D C_f/ZrC–SiC composites with PyC/SiC interphase before and after VSI are plotted in Fig. 1. A significant difference was found in the XRD patterns of the 3-D C_f/ZrC–SiC composites before and after VSI. The diffraction peaks mainly belong to C and ZrC before VSI, whereas diffraction peaks correspond to ZrC, SiC, Si, and C. The reaction between silicon vapor and carbon is dependent on the temperature of infiltration and the concentration of silicon vapor [14]. At 1700 °C, the silicon vapor became abundant. Some reacted with carbon forming SiC matrix, and the rest remained in the matrix. The forming SiC also made the density and open porosity in Table 1 reasonable.

At 1700 °C, a larger amount of vapor silicon reacted with the carbon and resulted in denser composites with better physical and mechanical behavior when the interphases were deposited, as shown in Table 2. The samples with interphases had a higher density, showing that relatively dense matrix can be achieved by VSI. Only a small difference was noted in their open porosity. It is also concluded that VSI is effective method to density the composites, and that the composites have good mechanical properties when the interphases are deposited.

The micrographs of polished cross-sections and EDS analysis for composites without interphase before and after VSI are shown in Fig. 2. It is obvious that some pores are observed not only in the intrabundle areas but also in the interbundle areas for the composite before VSI. However, for the composite after VSI, the interbundle area shows densified microstructure even though some closed micropores are observed in the intrabundle areas as shown in Fig. 2(b). As we know, it was found that fibers within a yarn were adhering to each other, resulting in the formation of closed micropores after impregnation. Thus, during the VSI process, the silicon vapor is difficult to infiltrate into the closed micropores in the intrabundle areas. Fig. 2 also shows the EDS analyses of a composite fabricated by the VSI process. Based on the EDS analyses, it shows the presence of Zr and C before VSI and Zr, C and Si after VSI. It is indicated that SiC matrix is formed and that the

Table 2
Properties of 3-D C_f/ZrC–SiC composites with different interphases.

Interphase	Fiber fraction	ZrC fraction	Density (g/cm^3)	Open porosity	Bending stress (MPa)	Elastic modulus (GPa)
None	28 vol%	26 vol%	2.01	10%	121 ± 13	17 ± 2.0
PyC	27 vol%	22 vol%	2.20	8%	221 ± 27	23 ± 3.0
PyC/SiC	25 vol%	24 vol%	2.25	6%	301 ± 15	25 ± 4.0

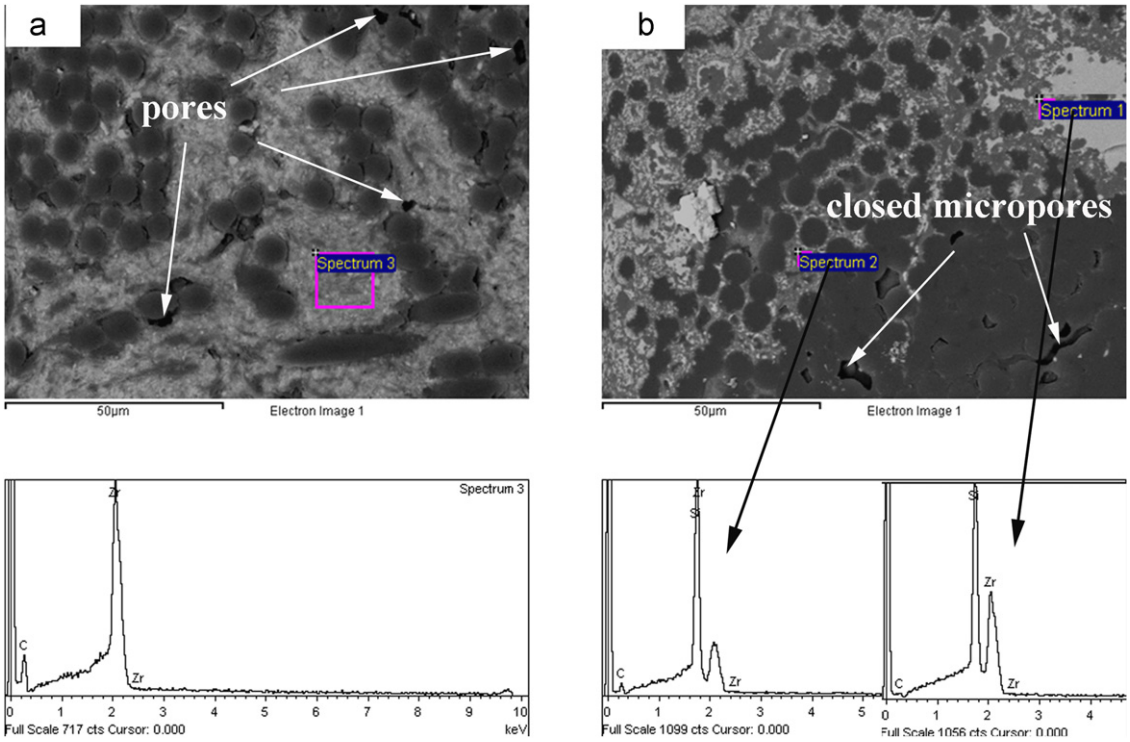

Fig. 2. SEM micrographs on the polished cross-section of 3-D C_f/ZrC–SiC composite without interphase: (a) before VSI and (b) after VSI.

residual Si existed after the VSI process according to the EDS analyses (Fig. 2) and the XRD patterns of the composites (Fig. 1). The residual Si in composites is attributed to the silicon vapor condensation during the cooling of the VSI process. When there are no interphases between the carbon fiber and matrix, the silicon vapor reacts not only with the carbon matrix, but also with carbon fibers, as shown in Fig. 2(b).

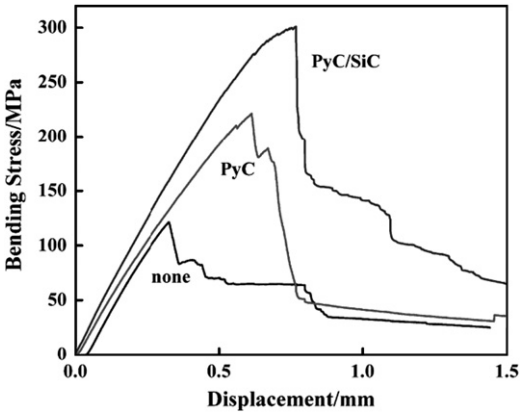

Fig. 3. Bending stress/displacement curves of 3-D C_f/ZrC–SiC composites with different interphases.

The bending stress–displacement curves of all the composites with different interphases are shown in Fig. 3. Based on these curves, all samples showed a typical non-brittle fracture behavior regardless of the existence of interphases. With the deposition of interphases, mechanical properties including elastic modulus and bending stress increased. This result is consistent with the data listed in Table 2. As mentioned before, the reaction between carbon fiber and silicon could decrease the fiber strength and increase the bonding strength between fiber and matrix.

The morphologies of fracture surfaces are shown in Fig. 4. It can be seen that all the composites showed a typical non-brittle fracture behavior, and fiber pullouts accompanied the fracture process. When no interphase was deposited, short pulled-out fibers with rather coarse surfaces can be observed. By contrast, with PyC/SiC or PyC interphases, longer pulled-out fibers with smoother surfaces can be observed. This phenomenon can be explained by the reaction between the fibers and the silicon vapor. When no interphase was deposited, silicon vapor reacted with the fibers, which damaged the fiber surfaces. As a result, some matrices evenly clung to the pulled-out fibers. However, the fibers can be protected from reacting with silicon vapor at such high temperature. As shown in Fig. 4(b) and (c), the fiber surfaces remained intact, and crack deflection parallel to the fiber axis can also be detected.

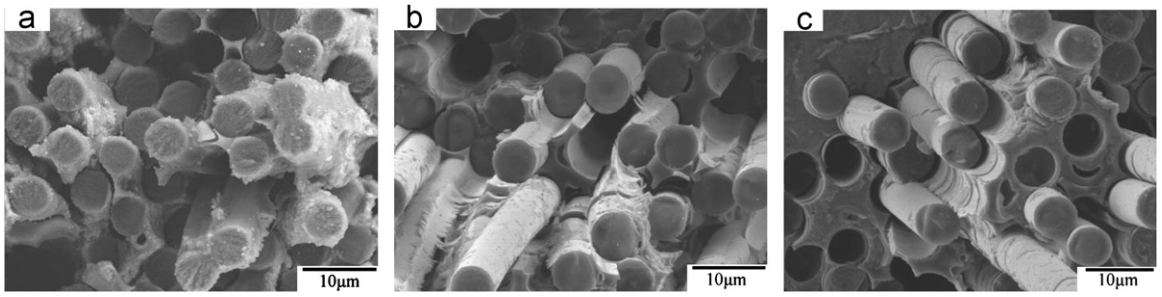

Fig. 4. SEM micrographs on the fracture surfaces of 3-D C_f/ZrC–SiC composites: (a) none, (b) PyC and (c) PyC/SiC.

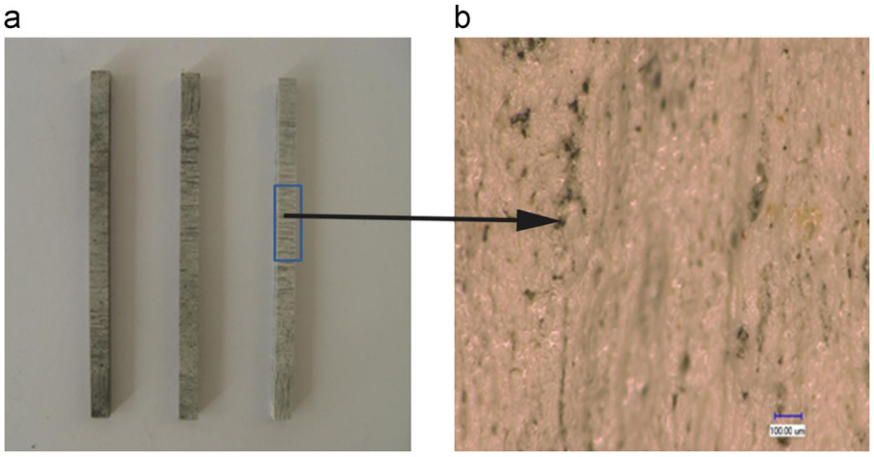

Fig. 5. Optical images of 3-D C_f/ZrC–SiC composites after oxidation: (a) after oxidation and (b) larger magnification.

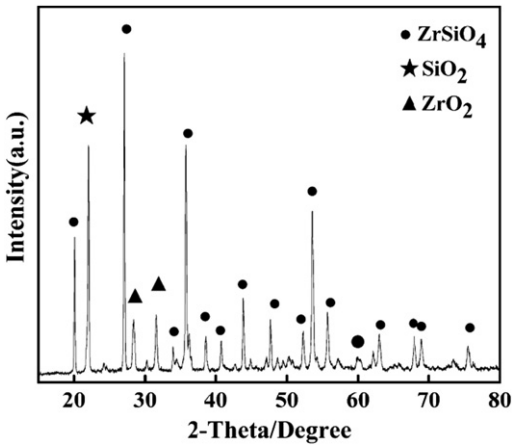

Fig. 6. XRD pattern of 3-D C_f/ZrC–SiC composite surface after oxidation.

The high temperature property of the C_f/ZrC–SiC composite is important. Hence, the oxidation resistance of the composites was evaluated through static oxidation at 1700 °C for 15 min in a muffle furnace. The optical images and XRD patterns of the 3-D C_f/ZrC–SiC composite after oxidation are shown in Figs. 5 and 6, respectively. As shown in Fig. 5(a), the shape of the 3-D C_f/ZrC–SiC composite after oxidation remained intact and the surface was totally covered with oxide. As shown in Figs. 5(b) and 6, a glass layer of $ZrSiO_4$ was formed when used in oxidative atmosphere. The phases include $ZrSiO_4$, SiO_2, and ZrO_2. The glass layer of $ZrSiO_4$ would prevent the composite from further oxidation. Meanwhile, the mass loss and linear recession rate of the C_f/ZrC–SiC composites exposed to oxyacetylene torch were 0.013 g/s and 0.004 mm/s, respectively. Compared with our previous research results [15,16], the mass loss and linear recession rate of the C_f/ZrC–SiC composites are almost the same. Therefore, 3-D C_f/ZrC–SiC composites have excellent high-temperature properties.

4. Conclusions

Three-dimensional C_f/ZrC–SiC composites were fabricated via the VSI process. The bulk density, open porosity, and flexural strength of the composite with PyC/SiC interphases were 2.25 g/cm^3, 6%, and 301 MPa, respectively. All composites exhibited a non-brittle failure behavior. Based on the oxidation resistance and ablation test through oxyacetylene torch, the results indicate that 3-D C_f/ZrC–SiC composites have excellent high-temperature properties.

Acknowledgments

Authors appreciate the financial support of the National Natural Science Foundation of China under the Grant nos. of 51172256 and 51142010.

References

[1] S. Schmidt, S. Beyer, H. Knabe, H. Immich, R. Meistring, A. Gessler, Advanced ceramic matrix composite materials for current and future propulsion technology applications, Acta Astronautica 55 (2004) 409–420.
[2] W. Krenkel, B. Heidenreich, R. Renz, C/C–SiC Composites for advanced friction systems, Advanced Engineering Materials 4 (2002) 427–436.
[3] S. Raffaele, D.S.F. Mario, S. Laura, S. Diletta, Arc-jet testing on HfB_2 and HfC-based ultra-high temperature ceramic materials, Journal of the European Ceramic Society 28 (2008) 1899–1907.
[4] R.L. Stanley, J.O. Elizabeth, C.H. Michael, D.K. James, S. Mrityunjay, A.S. Jonathan, Evaluation of ultra-high temperature ceramics for aeropropulsion use, Journal of the European Ceramic Society 22 (2002) 2757–2767.
[5] P. Lee, Y. Katoh, A. Kohyama, Microstructure analysis and strength evaluation of reaction sintered SiC/SiC composites, Scripta Materialia 44 (1) (2001) 153–157.
[6] G. Morscher, Stress-dependent matrix cracking in 2D woven SiC-fiber reinforced melting-infiltrated SiC matrix composites, Composites Science Technology 64 (9) (2004) 1311–1319.
[7] E. Vogli, H. Sieber, P. Greil, Biomorphic SiC-ceramic prepared by Si-vapor phase infiltration of wood, Journal of the European Ceramic Society 22 (14–15) (2002) 2663–2668.
[8] Y. Chiang, R. Messner, C. Terwilliger, Reaction-formed silicon carbide, Materials Science Engineering A 144 (1–2) (1991) 63–74.
[9] Q. Zhou, S.M. Dong, X.Y. Zhang, Y.S. Ding, D.L. Jiang, Fabrication of C_f/SiC composites by vapor silicon infiltration, Journal of the American Ceramic Society 89 (7) (2006) 2338–2340.
[10] Q.G. Li, S.M. Dong, Z. Wang, P. He, H.J. Zhou, J.S. Yang, B. Wu, J.B. Hu, Fabrication and properties of 3-D C_f/SiC–ZrC composites, using ZrC precursor and polycarbosilane, Journal of the American Ceramic Society 94 (4) (2012) 1216–1219.
[11] Q.G. Li, H.J. Zhou, S.M. Dong, Z. Wang, P. He, J.S. Yang, B. Wu, J.B. Hu, Fabrication of a ZrC–SiC matrix for ceramic matrix composites and its properties, Ceramics International 38 (2012) 4379–4384.
[12] Y.Z. Zhu, Z.R. Huang, S.M. Dong, M. Yuan, D.L. Jiang, Fabricating 2.5D SiC_f/SiC composite using polycarbosilane/SiC/Al mixture for matrix derivation, Journal of the American Ceramic Society 90 (3) (2007) 969–972.
[13] Q. Zhou, S.M. Dong, Y.S. Ding, Z. Wang, Z.R. Huang, D.L. Jiang, Three-dimensional carbon fiber-reinforced silicon carbide matrix composites by vapor silicon infiltration, Ceramics International 35 (2009) 2161–2169.
[14] Y. Wang, The preparation of reaction-formed SiC/Si composite from controllable porous carbon by Si infiltration, Ph.D. Thesis, Institute of Graduate, Chinese Academy of Sciences, China (in Chinese), 2004.
[15] Qinggang Li, Haijun Zhou, Shaoming Dong, Zhen Wang, Jinshan Yang, Bin Wu, Jianbao Hu, Fabrication and comparison of 3D C_f/ZrC–SiC composites using ZrC particles/polycarbosilane and ZrC precursor/polycarbosilane, Ceramics International 38 (6) (2012) 5271–5275.
[16] Qinggang Li, Shaoming Dong, Ping He, Haijun Zhou, Zhen Wang, Jinshan Yang, Bin Wu, Jianbao Hu, Mechanical properties and microstructures of 2D C_f/ZrC–SiC composites using ZrC precursor and polycarbosilane, Ceramics International (2012) 〈http://dx.dio.org/10.1016/j.ceramint.2012.04.005〉.